129. Physicochemical Properties of Deuterated Compounds

8th Communication[1])

The Kinetic Isotope Effect for the Reaction of Hydrogen Atoms with Methylcyclohexane and Perdeuteromethylcyclohexane in the Gas Phase

by **Noboru Fujisaki, Amanz Ruf,** and **Tino Gäumann***

Institute of Physical Chemistry, Federal Institute of Technology, CH-1015 Lausanne

(17.IV.85)

Using H-atoms produced in the radiolysis of water vapour, we determined the kinetic isotope effect for the reaction

$$H\cdot + RH(R'D) \xrightarrow{k_H/k_D} H_2(HD) + R\cdot(R'\cdot)$$

where RH and R'D are methylcyclohexane and perdeuterated methylcyclohexane, respectively. The result obtained from the isotope competitive method can be expressed with the *Arrhenius*-type equation $k_H/k_D = (0.51 \pm 0.04) \exp[(8.58 \pm 0.25)\ \text{kJ mol}^{-1}/RT]$ over the temperature range from 363 to 483 K. The occurrence of H abstraction from primary, secondary, and tertiary C–H bonds in methylcyclohexane is taken into consideration in the interpretation of the *Arrhenius*-type expression obtained. Theoretical interpretation of the kinetic isotope effect has been achieved on the basis of the transition-state theory and a semiempirical *London-Eyring-Polanyi-Sato* potential-energy surface. The tunnel effect is found to play a role in the H-abstraction. Several methods for estimating the tunnel correction factors have been discussed.

1. Introduction. – The H-atom is known to play an important role in the photolysis [1] [2], radiolysis [3] [4], and combustion processes [5] of hydrocarbons. The *Arrhenius* parameters for the reaction of H-atoms with organic compounds have been measured by various methods [6–10] and tabulated [11] [12].

We have been particularly interested in the study of the H/D kinetic isotope effects for the reactions of H-atoms with alkanes, since it provides considerable insight into reaction mechanisms. The kinetic isotope effect (KIE) is usually explained within the frame work of transition-state theory [13–16(a)]. To interpret the KIE, we need to invoke such terms as the potential-energy surface of a reacting system, vibrational frequencies of reactants and activated complexes, and tunnel corrections [16(b)–20]. In other words, the study of the KIE enables these terms to be discussed to some extent.

We have already determined the KIEs for the reactions of H-atoms with some saturated hydrocarbons [21–23] using radiolysis of water vapour [24] as the source of H-atoms. As a further extension, the KIE for H abstraction from methylcyclohexane has been undertaken in this work.

[1]) 7th Communication: *Helv. Chim. Acta* **1985**, *68*, 1160.

2. Experimental. – 2.1. *Materials.* Triply distilled H_2O was available from our previous works [21–23] [25] [26]. Research-grade methylcyclohexane was obtained from *Phillips Petroleum.* Perdeuterated methylcyclohexane was produced in a home-made reactor [27]. Both nondeuterated and perdeuterated methylcyclohexane were purified with prep. GC using a 5-m column of *Igepal CO 880* on Kieselgur. The isotopic purity of the (D_{14})methylcyclohexane was determined by MS to be > 99 atom-% D.

2.2. *Irradiation and Product Analysis.* The mole fractions of the (D_{14})methylcyclohexane in the nondeuterated methylcyclohexane and (D_{14})methylcyclohexane mixtures were usually 0.61, 0.71, 0.80, and 0.89. In typical runs, 0.50 g of H_2O and 12 mg of the hydrocarbon mixture were transferred into a *Pyrex* spherical vessel of 540 ml provided with a break seal after degassing the samples. The samples were irradiated in a ^{60}Co-γ-ray source *(Gammacell 220)* at a dose rate of 5.2 kGy/h to a total dose of 5.0 kGy. Unless otherwise specified, the samples were irradiated at 363, 393, 423, 453, and 483 K. The isotopic hydrogen formed was collected with a *Toepler* pump and subsequently analysed at 77 K by GC [28] using Ne as the carrier gas. In some experiments, radiolysis products other than hydrogen were also analysed by GC on a column packed with *Igepal CO 880.*

3. Results. – 3.1. *Reaction Mechanism.* Since the mechanism for the radiolysis of water vapour has been described in detail in [21] [24] [25], a brief account of them will be given here. Excitation and ionisation of water vapour by radiation lead to the formation of H_2O^*, H_2O^+; and e^- in the initial steps. The excited water molecules decompose to give H·, O, OH· radicals, and hydrogen molecule is eliminated in a unimolecular mechanism. The ion/molecule reaction of the ionised water molecule with water yields an OH· radical and a hydronium ion, H_3O^+. The hydration of the hydronium ion and subsequent neutralization of the hydrated hydronium ion by an electron results in H· and water molecule. To summarise, the radiolysis of water vapour may be depicted as follows:

$$H_2O \longrightarrow H\cdot, OH\cdot, O, H_2 \tag{1}$$

H_2 refers to the hydrogen formed in a unimolecular reaction. The formation of both O-atom and the H_2 are of minor importance here [21] [24]. Although the H· and OH· radicals are produced with comparatively large yields [21] [24], *i.e.*, $G(H\cdot) \approx G(OH\cdot) \approx 7$, they effectively undergo back reactions in the radiolysis of pure water vapour so that the G value for stable end products from pure water vapour is very small [21] [24], *i.e.*, < 0.2.

In the presence of a small concentration of methylcyclohexane and its deuterated counterpart denoted by RH and R'D, the H· and OH· radicals produced in *Reaction 1* will efficiently abstract a hydrogen or deuterium atom from the additives at temperatures > 360 K.

$$H\cdot + RH \xrightarrow{k_H} H_2 + R\cdot \tag{2}$$

$$H\cdot + R'D \xrightarrow{k_D} HD + R'\cdot \tag{3}$$

$$OH\cdot + RH \longrightarrow H_2O + R\cdot \tag{4}$$

$$OH + R'D \longrightarrow HDO + R'\cdot \tag{5}$$

$$R\cdot + R\cdot \longrightarrow RH + R(-H) \tag{6}$$

$$R\cdot + R\cdot \longrightarrow R{-}R \tag{7}$$

In the case where cyclohexane was taken as an additive, the main products were identified to be hydrogen, cyclohexene, and bicyclohexyl. Furthermore, the material balance expected from the reaction scheme, G(hydrogen) = G(cyclohexene) + G(bicyclohexyl), was confirmed [25] [26].

With methylcyclohexane, the radical R· produced in *Reactions 2* and *4* represents five isomeric radical species, *i.e.* cyclohexylmethyl, 1-, 2-, 3-, and 4-methylcyclohexyl radicals. The disproportionation and combination of these radicals lead to the formation of methylidenecyclohexane, 1-, 3-, and 4-methylcyclohexene, and various dimeric isomers, all of which were in fact found by GC to be the main products. However, a limited effort was made to quantitatively measure their yields.

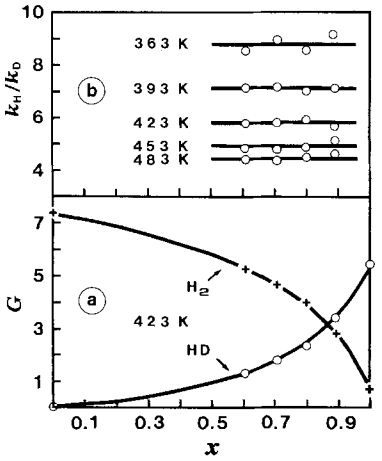

Fig. 1. (a) G *value for* H_2 *and HD formed in the gas-phase radiolysis of* H_2O + *(methylcyclohexane +* (D_{14})*methylcyclohexane) mixtures as a function of* x, *where* x = [(D_{14})methylcyclohexane]/{[methylcyclohexane] + [(D_{14})methylcyclohexane]}. G (D_2), not shown, is less than 0.10 over the whole range of x. Dose = 5.0 kGy, $p = 1.80 \times 10^5$ Pa, $V = 0.54$ l, the total concentration of the added methylcyclohexane = 0.45 mol-%. (b) *The KIEs at various temperatures calculated from* Eqn. 10.

3.2. *Determination of the KIE. Fig. 1(a)* shows the yields of H_2 and HD evolved from the mixtures of water vapour with methylcyclohexane as a function of x, where $x = [R'D]/\{[RH] + [R'D]\}$. The G value for H_2 and HD in *Fig. 1(a)* can be represented [21–23] by *Eqns. 8* and *9*, respectively,

$$G(H_2) = g(H_2) + g(H)\frac{k_H[RH]}{k_H[RH] + k_D[R'D] + k_Y[Y]} \tag{8}$$

$$G(HD) = g(H)\frac{k_D[R'D]}{k_H[RH] + k_D[R'D] + k_Y[Y]} \tag{9}$$

where the measured yields are denoted by G, and the primary yields in water vapour by g. The $g(H_2)$ corresponds to the g value for the molecular hydrogen. The term k_Y [Y] means that the additives compete for H-atoms with some reaction intermediates or stable products formed. Rearrangements of *Eqns. 8* and *9* give

$$\frac{k_H}{k_D} = \frac{G(H_2) - g(H_2)}{G(HD)} \cdot \frac{[R'D]}{[RH]} = \frac{G(H_2) - g(H_2)}{G(HD)} \cdot \frac{x}{1 - x} \tag{10}$$

which permits the k_H/k_D value to be calculated as a function of x. *Fig. 1(b)* shows the isotope effects at different temperatures calculated from *Eqn. 10*. The ratios k_H/k_D are independent of the ratios [R'D]/[RH] over a wide range, indicating the validity of *Eqn. 10*.

The use of *Eqn. 10* implicitly assumes [21–23] that the experiments were carried out under the following conditions: *i*) the conversion of RH and R'D is low, *ii*) the H_2 and HD formed in *Reactions 2* and *3* do not undergo further reactions, and *iii*) the direct decomposition of the additive to give H- and D-atoms is negligible. Our experimental conditions were chosen so as to meet the above requirements. Since the values of KIE have been measured as a function of temperature *(Fig. 1(b))*, the ratio A_H/A_D and the difference in activation energy $E_D - E_H$ were obtained from the least-squares treatment of the experimental data. The results are summarised in *Table 1* along with the data previously determined for the reactions of H-atoms with neopentane, cyclohexane, and isobutane [21–23]. The bond strengths of the primary, secondary, and tertiary C–H bonds in neopentane, cyclohexane, and isobutane decrease in this order. The $E_D - E_H$ values decrease in going from neopentane through cyclohexane to isobutane, indicating that the stronger the C–H bond the larger the $E_D - E_H$ value. Contrary to this, the pre-exponential factor ratios A_H/A_D increase in going from neopentane to isobutane.

4. Discussion. – 4.1. *Additivity of Rate Constants.* It is conceivable that abstraction of an H-atom by H-atoms takes place from primary, secondary, and tertiary C–H bonds in methylcyclohexane. Then, the overall rate constant k_H for *Reaction 2* can be expressed as the sum of rate constants [5] [29] [30].

$$k_H = n_p k_H^p + n_s k_H^s + n_t k_H^t \tag{11}$$

In this, k_H^p, k_H^s and k_H^t are the intrinsic rate constants per C–H bond for abstraction of H from the primary, secondary, and tertiary C–H bonds, respectively, and n_p, n_s and n_t stand for the number of the primary, secondary, and tertiary C–H bonds in the alkane. From an analysis of comprehensive kinetic data for the reaction of H-atoms with alkanes, *Baldwin* and *Walker* [5] derived the following values for k_H^p, k_H^s, and k_H^t in units of $dm^3\ mol^{-1}\ s^{-1}$;

$$k_H^p = 2.2 \times 10^{10} \exp[-39.2\ \text{kJ mol}^{-1}/RT],$$
$$k_H^s = 4.9 \times 10^{10} \exp[-33.3\ \text{kJ mol}^{-1}/RT], \tag{12}$$

and
$$k_H^t = 5.1 \times 10^{10} \exp[-25.2\ \text{kJ mol}^{-1}/RT]$$

An alternative formula, due also to *Baldwin* and *Walker* [5], leads essentially to the same conclusion in the following calculations. Recent studies show that the *Arrhenius* plots, which are concave upwards, are obtained when the logarithm of the rate constants for the reactions of H-atoms with ethane [8] and propane [6] are plotted *vs.* $1/T$ over a broad temperature range. This may mean that the generalised rate constants *(Eqn. 12)* are valid for limited temperature ranges, and they may indicate that the tunnel effect [19] is involved in the H-abstraction reactions.

The rate constant associated with abstraction of a D-atom from perdeuterated methylcyclohexane can also be represented by the equation similar to *Eqn. 11*,

$$k_D = n_p k_D^p + n_s k_D^s + n_t k_D^t \tag{13}$$

Therefore, the values of the KIE for methylcyclohexane calculated from *Eqn. 10* can be re-expressed as follows:

$$\frac{k_H}{k_D} = \frac{n_p k_H^p + n_s k_H^s + n_t k_H^t}{n_p k_D^p + n_s k_D^s + n_t k_D^t} \tag{14}$$

Neopentane contains only primary H-atoms, so that the KIE for neopentane listed in *Table 1* is considered to be the intrinsic KIE, k_H^p/k_D^p, for abstraction of the primary H-atom. In a similar fashion, the KIE for cyclohexane having only secondary C–H bonds is taken to be k_H^s/k_D^s, the KIE inherent to abstraction from the secondary C–H bond. Abstraction of H from isobutane may occur both from primary and from tertiary C–H bonds. However, adopting the rate constants quoted in *Eqn. 12*, one can estimate the contribution from the tertiary H-atom to the total rate of H-abstraction to be *ca.* 93% at the middle of the presently used temperature range, 423 K. Thus H-abstraction from isobutane takes place dominantly from the tertiary C–H bond. Consequently, the KIE for isobutane shown in *Table 1* is taken to represent the specific KIE, k_H^t/k_D^t, for abstraction from the tertiary C–H bond to a first approximation.

Table 1. *Experimental KIEs for Abstraction of H- and D-Atoms from Alkanes by H-Atoms*

Reaction	k_H/k_D[a])		Temp. range	Ref.
	A_H/A_D	$(E_D - E_H)$ [kJ mol^{-1}]	[K]	
H + neopentane/(D_{12})neopentane[b])	0.32 ± 0.04	11.0 ± 0.5	373–483	23
H + cyclohexane/(D_{12})cyclohexane	0.43 ± 0.03	9.7 ± 0.2	363–463	22
H + cyclohexane/(D_{12})cyclohexane	0.41 ± 0.05	9.6 ± 0.4	353–493	21
H + isobutane/(D_{10})isobutane	0.60 ± 0.11	7.8 ± 0.6	373–463	23
H + methylcyclohexane/(D_{14})methylcyclohexane[c])	0.51 ± 0.04	8.6 ± 0.2	363–483	[d])

[a]) $k_H/k_D = A_H/A_D \exp[(E_D - E_H)\text{ kJ mol}^{-1}/RT]$.

[b]) Abbreviations of H· + neopentane $\xrightarrow{k_H}$ $H_2 + C_5H_{11}$ and H· + (D_{12})neopentane $\xrightarrow{k_D}$ $HD + C_5D_{11}$.

[c]) Methylcyclohexane.

[d]) This work.

Then, no unknown parameter is present in calculating the k_H/k_D values by means of the right-hand side of *Eqn. 14*, since the intrinsic rate constants k_H^p,k_H^s, and k_H^t are given by *Eqn. 12*, and the intrinsic KIEs k_H^p/k_D^p, k_H^s/k_D^s, and k_H^t/k_D^t are available fom *Table 1*. The KIE calculated from *Eqn. 14* is compared in *Fig. 2* with experimental data. Good agreement is obtained. We acknowledge that the characteristic rate constants and KIEs for primary, secondary, and tertiary C–H bonds in methylcyclohexane may slightly

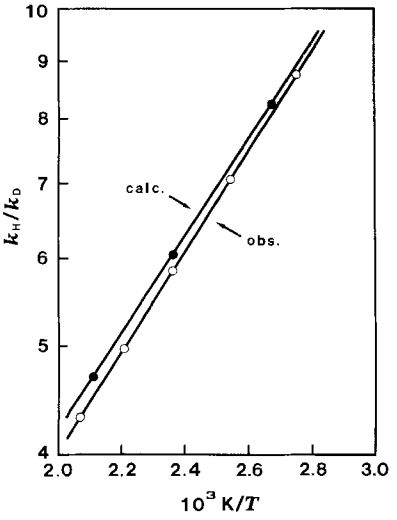

Fig. 2. *The* k_H/k_D *values for H· + methylcyclohexane/(D_{14})methylcyclohexane* vs. *the reciprocal of the absolute temperatures.* (○); observed, (●); calculated from *Eqn. 14*.

differ from those for the primary, secondary, and tertiary C–H bonds in neopentane, cyclohexane, and isobutane. The slight differences are, however, not detectable, when the experimental k_H/k_D values are compared with the calculated ones. As a conclusion, it seems possible to estimate the KIE for H-abstraction from complex alkanes, if both relevant rate constants and KIEs inherent to the primary, secondary, and tertiary H-atoms are known.

4.2. *Theoretical Calculation of the KIE* k_H^s/k_D^s. A theoretical interpretation of the KIE for the reaction of H-atoms with cyclohexane, k_H^s/k_D^s, has been reported in [22] [23]. However, various possible tunnel paths have not been considered. In the present calculations, emphasis is placed upon finding the relevant pathway through which tunnelling of the H-atom occurs. According to transition-state theory [13], the KIE is given [14–16(a)] by

$$\frac{k_H^s}{k_D^s} = \frac{\nu_{iH}}{\nu_{iD}}\left(\frac{\Gamma_H}{\Gamma_D}\right)^* \prod_{j=1}^{3N^{\neq}-7}\left(\frac{\Gamma_{Hj}}{\Gamma_{Dj}}\right)^{\neq} \prod_{j=1}^{3N-6}\left(\frac{\Gamma_{Dj}}{\Gamma_{Hj}}\right)^{r}\left(\frac{\sigma_H}{\sigma_D}\right) \tag{15}$$

where ν_i is the imaginary frequency corresponding to the motion along the reaction coordinate, Γ^* represents the tunnelling correction factor, $\Gamma_j^{\neq}$ and Γ_j^r denote quantum correction factors for each of real vibration of the activated complexes and the reactants, and are of the form,

$$\Gamma_j = (u_j/2)/\sinh(u_j/2)$$

with $u_j = h\nu_j/kT$; $N^{\neq}$ and N refer to the number of atoms in the activated complexes and the reactants, and σ stands for the reaction-path degeneracy.

Eqn. 15 is inconvenient for our problem, since if *Eqn. 15* were to be used, 48 and 51 vibrational frequencies have to be evaluated theoretically for the reactant cyclohexane and the activated complex, respectively. Although recent progresses in quantum mechanical calculations of vibrational frequencies for neutral molecules [31] and activated complexes [32] [33] are conspicuous, and are making it interesting to estimate rate constants in terms of transition-state theory, it seems us difficult to calculate 51 vibrational frequencies for the activated complex by quantum-mechanical methods.

So we adopt the drastically simplified collinear three-atom model

$$A + BC \rightarrow [A\text{---}B\text{---}C]^{\neq} \rightarrow AB + C.$$

In this case, *Eqn. 15* is reduced to

$$\frac{k_H^s}{k_D^s} = \frac{\nu_{iH}}{\nu_{iD}}\left(\frac{\Gamma_H}{\Gamma_D}\right)^* \left(\frac{\Gamma_{st.H}\Gamma_{b.H}^2}{\Gamma_{st.D}\Gamma_{b.D}^2}\right)^{\neq} \left(\frac{\Gamma_{st.D}}{\Gamma_{st.H}}\right)^{r} \tag{16}$$

where st. and b. refer to stretch and bending, respectively.

The first step in setting up the theoretical calculation is to construct the potential-energy surface for the particular reaction of interest. For this purpose, the semiempirical *London-Eyring-Polanyi-Sato* (LEPS) equation with a single adjustable parameter is applied [16(c)] [34] [35]. One can delineate the LEPS potential surface with a few physicochemical constants of reactant cyclohexane and product hydrogen. *Table 2* summarises some molecular properties necessary to the calculation. A portion of the LEPS surface is schematically displayed in *Fig. 3*. Standard analyses [16(d)] of the potential surface led to the vibrational frequencies for the activated complexes listed in *Table 3*. The vibrational frequencies in *Tables 2* and *3* enable the terms $\Gamma^{\neq}$ and Γ^r to be computed as a function of

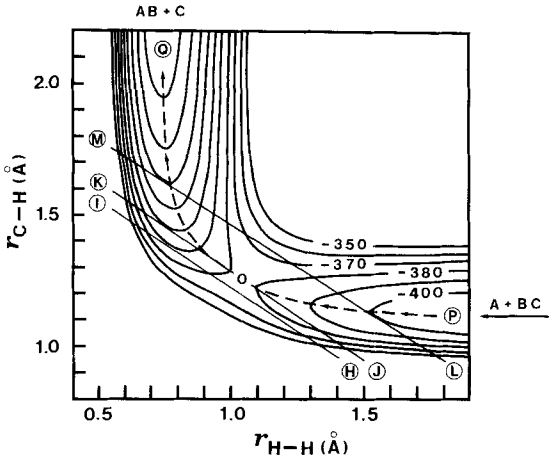

Fig. 3. *Potential-energy contour map for the collinear reaction H· + cyclohexane → H_2 + cyclohexyl· calculated according to the LEPS method.* The contour lines are at 10 kJ mol^{-1} intervals. The broken line POQ represents the reaction path, and the solid line JOK shows the reaction coordinate. The lines HI and LM are parallel to the line JOK.

Table 2. *Molecular Properties of Cyclohexyl–H and H–H*[a])

Property	Cyclohexyl–H	H–H
D°_{298} [kJ mol^{-1}]	399.57	431.56
$\tilde{\nu}_{st.}$ [cm^{-1}]	2933 (2206)[b])	4395.2
D_e [kJ mol^{-1}]	417.1	457.86
r_o [Å]	1.119	0.7417
β[c]) [Å^{-1}]	1.844	1.9420
ζ[d])	0.10	0.10

[a]) Taken from [23]. [b]) $\tilde{\nu}_{st.}$ for (D_1)–(D_{11}) cyclohexyl. [c]) *Morse* parameter. [d]) *Sato* parameter.

Table 3. *Properties of the Activated Complexes Calculated from the Aligned Three-Atom Model*[a]) *A + BC → AB + C*

Property	H···H···cyclohexyl	H···D···(D_{11})cyclohexyl
$V^{\neq}$ [kJ mol^{-1}]	38.014	38.014
$r^{\neq}_{AB}$ [Å]	1.0479	1.0479
$r^{\neq}_{BC}$ [Å]	1.2563	1.2563
$f^{\neq}_{AB}$ [mdyn/Å]	0.081	0.081
$f^{\neq}_{BC}$ [mdyn/Å]	1.433	1.433
$f^{\neq}_{AC}$ [mdyn/Å]	1.492	1.492
$f^{\neq}_{\theta}$ [10^{11} erg/rad^2]	0.073	0.073
$\tilde{\nu}_{st.}$ [cm^{-1}]	1334	1239
$\tilde{\nu}_{b.}$ [cm^{-1}]	704	554
$\tilde{\nu}_i$ [cm^{-1}]	1978i	1560i

[a]) Taken from [23].

temperature. Finally, we are faced with the tunnel correction terms Γ^* which remain to be estimated. The term Γ^* is in general given [16(b)] by

$$\Gamma^* = \frac{\int_0^{\infty} \kappa(\nu_i, V_1, V_2, E, T) \exp(-E/RT)\,dE}{\int_{V_1}^{\infty} \exp(-E/RT)\,dE} \tag{17}$$

where the barrier permeability $\varkappa$ is a function of the imaginary frequency ν_i, the potential well depths V_1 and V_2, total energy E of the system, and temperature T. The potential-energy profile plays the key role in the calculation of the tunnelling correction, because some important quantities such as ν_i, V_1, and V_2 emerge from it. Unfortunately, there are some ambiguities [16(c)] [17] [18] [22] as to how to delineate the energy profile. Hence, the three different cases are taken up among others for constructing the energy profile.

In *Case 1*, a cut of the LEPS potential surface was taken along the reaction coordinate JOK as show in *Fig. 3*. The straight line JOK is tangent to the minimum-energy path POQ at the saddle point 0. *Fig. 4* illustrates the unsymmetrical potential-energy curve emerged. The potential-well depths V_1 and V_2 are directly read off from *Fig. 4*.

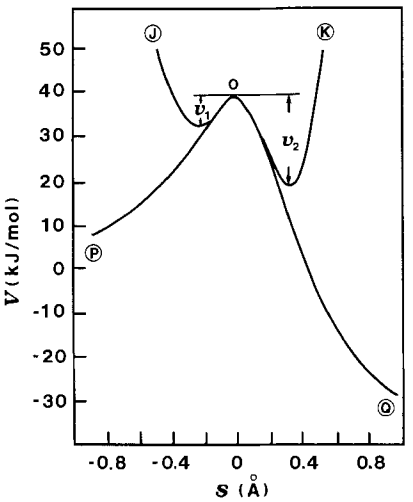

Fig. 4. *The LEPS potential-energy profiles along the reaction path POQ and along the reaction coordinate JOK in* Fig. 3 *as a function of distance* s *from the saddle point of the surface*

In *Case 2*, we chose the potential profile along the path of lowest energy POQ *(Fig. 3)*. This profile is also drawn in *Fig. 4*, and has been used as a reasonable tunnel path in our previous works [22] [23]. For *Case 2*, the zero-point energies (ZPEs) are taken into consideration in the calculation of V_1 and V_2, *viz.*,

$$V_1 = V^{\neq} + \text{ZPE (activated complex)} - \text{ZPE (reactant)}$$

$$V_2 = V^{\neq} + \text{ZPE (activated complex)} - \text{ZPE (product)} + \Delta D_e$$

where $V^{\neq}$ is the potential energy of activation in *Table 3*, and $\Delta D_e = D_e$ (product) $- D_e$ (reactant) (the values for D_e are shown in *Table 2*).

In *Case 3*, the tunnel paths are provided by cutting the LEPS surface in parallel to the reaction coordinate JOK at an interval of 0.01 Å. Straight lines HI and LM in *Fig. 3* are the examples of such parallel cuts. This procedure yields many potential-energy profiles with double-minimum as shown in *Fig. 5*. In this case, the tunnel factor Γ^* was first calculated from *Eqn. 17* for each parallel cut. Then, each value of Γ^* was multiplied by a *Boltzmann* factor $\exp(-\Delta V/RT)$, where the ΔV is the difference between the saddle-point energy and the maximum value of the parallel cut. *Fig. 6* shows the corrected tunnel coefficients, $\Gamma^* \exp(-\Delta V/RT)$, as a function of the distance of the tunnel path from the line JOK. The desired mean tunnelling factor $\bar{\Gamma}^*$ is given by

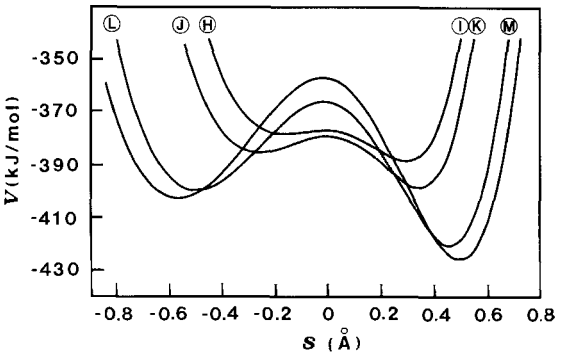

Fig. 5. *Some examples of the potential-energy profiles along the straight lines parallel to the reaction coordinate JOK as a function of distance* s *from the potential extrema*

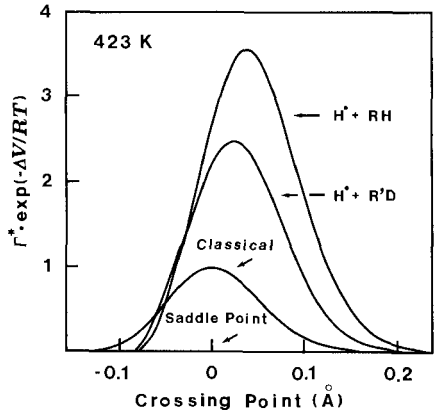

Fig. 6. *Corrected tunnel coefficients for various parallel cuts in* Fig. 3. $T = 423$ K.

$$\tilde{\Gamma}^* = \frac{\int \Gamma^* \exp(-\Delta V/RT)\,dr}{\int \exp(-\Delta V/RT)\,dr} \tag{18}$$

where r is the coordinate perpendicular to the reaction coordinate JOK. In order to calculate Γ^*, we have to convert in each case all the energy profiles in *Fig. 4* and *5* into the idealised *Eckart* barriers [20], for which the transmission coefficients $\varkappa$ can be computed exactly. *Table 4* lists the experimental and theoretical values for k_H^s/k_D^s. *Fig. 7* compares the calculated values of k_H^s/k_D^s with experimental ones. The experimental isotope effects agree rather well with the theoretical values calculated by using the tunnel factors for *Case 2*. The tunnel corrections of *Cases 1* and *3* lead to much smaller isotope effects than experiment. As a conclusion, the tunnel path considered in *Case 2* seems to be reasonable and legitimate. The invention of many tunnelling paths is in itself inconsistent with the tenet of transition-state theory, because transition-state theory assumes the existence of the unique reaction coordinate, for which the unique tunnel path is conceivable.

Table 4. *The KIE for the Reaction H· + Cyclohexane ((D12)Cyclohexane)* $\xrightarrow{k^s_H/k^s_D}$ H_2 (HD) + *Cyclohexyl· ((D11)Cyclohexyl·)*

T(K)	$(k^s_H/k^s_D)_{exptl.}$[a])	$(k^s_H/k^s_D)_{calcd.}$		
		Case 1	Case 2	Case 3
373	9.72	3.53	8.62	4.59
423	6.72	3.11	5.87	3.80
473	5.03	2.80	4.46	3.28

[a]) From [23].

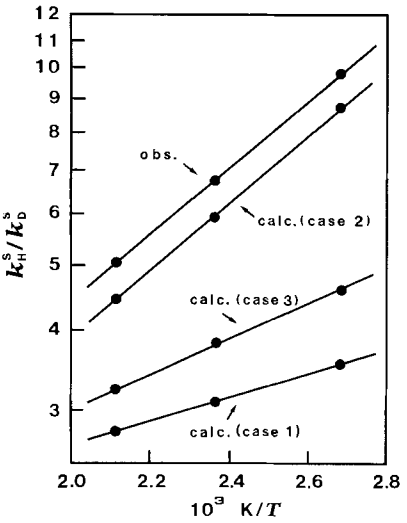

Fig. 7. *Observed and theoretically calculated kinetic isotope effects for H· + cyclohexane/(D12)cyclohexane* vs. *the reciprocal of the absolute temperature.* The tunnel coefficients estimated for *Cases 1, 2,* and *3* are used to calculate the theoretical values of the KIE.

In practice, the magnitude of the tunnel factors heavily depends on the *Sato* parameter ζ in *Table 2* used to construct the LEPS potential surface, and moreover, since we cannot give a sound physical meaning to the value of ζ chosen, search for the reasonable tunnel path remains to be continued further.

The authors thank Mrs. *M. Goël* for analyses of the isotopes of hydrogen. One of the authors *(N.F.)* acknowledges Prof. *Shin Sato* for helpful discussion. This work was supported by a grant from the *Swiss National Science Foundation.*

REFERENCES

[1] J.R. McNesby, H. Okabe, in 'Advances in Photochemistry', Eds. W.A. Noyes, Jr., G.S. Hammond, and J.N. Pitts, Jr., Interscience, New York, 1964, Vol. 3, pp. 157–240.

[2] P. Ausloos, S.G. Lias, in 'Chemical Spectroscopy and Photochemistry in the Vacuum Ultraviolet', Eds. C. Sandorfy, P.J. Ausloos, and M.B. Robin, Reidel, Dordrecht, 1974, pp. 465–482.

[3] N. Fujisaki, T. Gäumann, *Radiat. Phys. Chem.* **1984,** *23,* 49.

[4] I. György, in 'Radiation Chemistry of Hydrocarbons', Ed. G. Földiák, Elsevier, Amsterdam, 1981, pp. 61–175.

[5] R. R. Baldwin, R. W. Walker, *J. Chem. Soc., Faraday Trans. 1* **1979,** *75,* 140.
[6] R. M. Marshall, H. Purnell, A. Sheppard, *J. Chem. Soc., Faraday Trans. 1* **1984,** *80,* 2999.
[7] J. N. Bradley, K. O. West, *J. Chem. Soc., Faraday Trans. 1* **1976,** *72,* 8.
[8] J.-R. Cao, M. H. Back, *Can. J. Chem.* **1984,** *62,* 86.
[9] K. Hoyermann, A. W. Preuss, H. Gg. Wagner, *Ber. Bunsenges. Phys. Chem.* **1975,** *79,* 156.
[10] D. Mihelcic, V. Schubert, F. Höfler, P. Potzinger, *Ber. Bunsenges. Phys. Chem.* **1975,** *79,* 1230.
[11] W. E. Jones, S. D. MacKnight, L. Teng, *Chem. Rev.* **1973,** *73,* 407.
[12] J. A. Kerr, S. J. Moss, 'Handbook of Bimolecular and Termolecular Gas Reactions', C. R. C. Press, Boca Raton, Florida, 1981, Vol. 1.
[13] S. Glasstone, K. J. Laidler, H. Eyring, 'The Theory of Rate Processes', McGraw-Hill, New York, 1941.
[14] J. Bigeleisen and M. Wolfsberg, in 'Advances in Chemical Physics', Ed. I. Prigogine, Interscience, New York, 1958, Vol. 1, pp. 15–76.
[15] L. Melander, W. H. Saunders, Jr., Reaction Rates of Isotopic Molecules', Interscience, New York, 1980.
[16] H. S. Johnston, 'Gas Phase Reaction Rate Theory', Ronald, New York, 1966, (a) Chap. 13; (b) Chap. 2; (c) Chap. 10; (d) pp. 333, 339.
[17] H. S. Johnston, D. Rapp, *J. Am. Chem. Soc.* **1961,** *83,* 1.
[18] D. G. Truhlar, A. Kuppermann, *J. Am. Chem. Soc.* **1971,** *93,* 1840.
[19] R. P. Bell, 'The Tunnel Effect in Chemistry', Chapman and Hall, London, 1980.
[20] C. Eckart, *Phys. Rev.* **1930,** *35,* 1303.
[21] N. Fujisaki, T. Gäumann, *Ber. Bunsenges. Phys. Chem.* **1977,** *81,* 544.
[22] N. Fujisaki, A. Ruf, T. Gäumann, *J. Chem. Phys.* **1984,** *80,* 2570.
[23] N. Fujisaki, A. Ruf, T. Gäumann, *J. Am. Chem. Soc.* **1985,** *107,* 1605.
[24] R. S. Dixon, *Radiat. Res. Rev.* **1970,** *2,* 237.
[25] N. Fujisaki, T. Gäumann, *Int. J. Chem. Kinet.* **1979,** *11,* 345.
[26] N. Fujisaki, T. Gäumann, *Int. J. Chem. Kinet.* **1982,** *14,* 1059.
[27] T. Gäumann, H. Öz, O. Piringer, *Helv. Chim. Acta* **1978,** *61,* 258.
[28] T. Gäumann, O. Piringer, A. Weber, *Chimia* **1970,** *24,* 112.
[29] N. R. Greiner, *J. Chem. Phys.* **1970,** *53,* 1070.
[30] K. R. Darnall, R. Atkinson, J. N. Pitts, Jr., *J. Phys. Chem.* **1978,** *82,* 1581.
[31] K. B. Wiberg, R. C. Dempsey, J. J. Wendoloski, *J. Phys. Chem.* **1984,** *88,* 5596.
[32] S. B. Brown, M. J. S. Dewar, G. P. Ford, D. J. Nelson, H. S. Rzepa, *J. Am. Chem. Soc.* **1978,** *100,* 7832.
[33] G. C. Schatz, A. L. Wagner, T. H. Dunning, Jr., *J. Phys. Chem.* **1984,** *88,* 221.
[34] S. Sato, *J. Chem. Phys.* **1955,** *23,* 592, 2465.
[35] R. E. Weston, Jr., *J. Chem. Phys.* **1959,** *31,* 892.